ACOUSTICS 2012

Design and fabrication of an acoustic bragg mirror for miniaturized quartz resonators

E. Lebrasseur, T. Baron, S. Alzuaga, J.-J. Boy, L. Couteleau and S. Ballandras

Femto-st, Département Temps-Fréquence, 26 Chemin de l'Epitaphe, 25030 Besançon, France
thomas.baron@femto-st.fr

The use of a Bragg mirror for the confinement of the energy in the resonator appears nowadays as a promising way to achieve monolithic resonators, with simplified packaging, free of the constraint effects induced by the traditional quartz cases and free of low resonant frequencies disturbances. Moreover, this approach offers the possibility of batch processing on four inches wafers. The expected benefits are a reduction of the quartz layer thickness, a rigid holding from the backside of the device, and the transfer of the electrical connections to the topside only. The packaging is further simplified by the fact that only the topside needs to be encapsulated, for instance by quartz bonding technology. In this work we present the design and fabrication of an acoustic Bragg mirror used to enhance the performances of traditional quartz resonators. The best materials configurations are determined by simulations and the mirror is fabricated by wafer bonding technology based on metallic compression.

1 Introduction

Quartz is the best suited material to produce ultra stable (at 5 to 10 MHz) or high spectral purity (around 100 MHz) oscillators, both for military and space markets. The most optimized high performance, severe conditions quartz resonator version is the BVA ("Boitier à Vieillissement Amélioré": Improved ageing package), which was developed 30 years ago by R. Besson. BVA technology did not perform evolution since then, as, at the same time, electronic continuously moved toward increasing integration and miniaturization.

In order to remain a mandatory material, quartz has to follow the same way. This work is focusing on this objective. Conditions are fulfilled now: On one hand, multi applications simulation tools are now ready to fully implement quartz modeling. On the other hand, innovative technological processes, such as micro-machining, multi-layer assembly or wafer bonding, can be successfully applied to quartz, in order to miniaturize packaged resonators while optimizing their performances.

One of the main issues to fabricate a high performance quartz resonator is the holding. The state of the art is a holding in two points or four points at the rim of the resonator body, at low sensitive positions. In this work we propose to hold the resonator directly on one face by using an acoustic Bragg mirror. The electrical connection with the other components (printed circuit board, ceramic, etc.) is done on the opposite face by wire bonding.

2 Concept

The concept was proposed in 1965 by Newell at the Westinghouse Laboratories [1]. He was mentioning the difficulties in the fabrication of good quality bonding between quarter-wave plates, which is the essential condition for the correct functioning.

Using a Bragg mirror to confine the energy in the resonator [2] seems a promising way to fabricate monolithic resonators, with simplified case, free from the constrains effects induced by the traditional "quartz" cases and free from the low frequencies resonances. Moreover, this approach is compatible with batch processing on wafers. An example of such structure is presented in Figure 1, showing the basic concept as well as the admittance response predicted by a simplified yet rigorous calculation [3].

In the next paragraph, we present the simulations that lead us to define the most suitable materials for the design of a Bragg Mirror working at a frequency of 10Mhz.

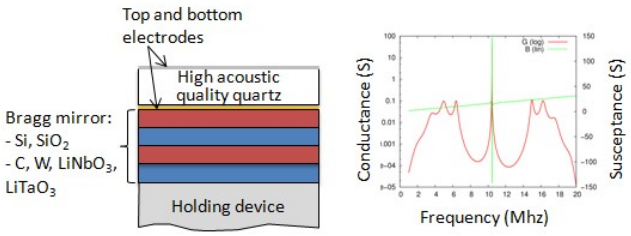

Figure 1: Basic concept of the Bragg Mirror: a) the structure b) calculated admittance response

3 Simulations

This section presents a comprehensive calculation of reflection and transmission coefficients of a layered structure accounting for any kind of polarization (longitudinal, pure shear, quasi-polarizations). The only restrictions are related to the perfect parallelism and planar nature of the interfaces within the material stack as well as the assumption of a perfect mechanical coupling between the adjacent layers.

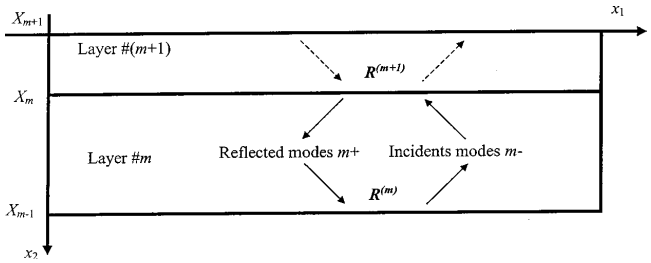

Figure 2: Definition of incident and reflected waves at the interface between layers m and m+1

According to Fahmy-Adler approach [4], we consider a state vector $\mathbf{h} = (u_i, T_{2j})^t$ associating the generalized stress and displacement fields to describe the acoustic behavior of each material of the stack by an eigenvalue problem (the upper-script t indicates vector or matrix transposition). The stacked structure conforms to the definition of Figure 2. For a given couple of slowness (s_1, s_3), the state vector for any material of the layer stack can be expressed as the product of a matrix $\mathbf{F}$ composed of the 8 corresponding eigen-vectors with a diagonal matrix $\mathbf{\Delta}(x_2)$ of rank 8×8 describing the dependence along x_2 via the eigenvalues s_2 and a vector $\mathbf{a}$ of the partial mode amplitudes:

$$\mathbf{h}(x_2) = \mathbf{F}\mathbf{\Delta}(x_2)\mathbf{a}e^{2j\pi f(t - s_1 x_1 - s_3 x_3)} \quad (1)$$

For each layer m, an intermediate variable $\mathbf{g}^{(m)}$ is introduced. This vector of same nature and rank as **a** allows for the separation of reflected and incident partial waves at the layer interfaces (see Figure 2):

$$\mathbf{g}^{(m)}(x_2) = \begin{pmatrix} \mathbf{g}^{(m+)} \\ \mathbf{g}^{(m-)} \end{pmatrix} = \boldsymbol{\Delta}^{(m)}(x_2)\mathbf{a}^{(m)} = \tag{2}$$

$$\begin{pmatrix} \boldsymbol{\Delta}^{(m+)}(x_2) & 0 \\ 0 & \boldsymbol{\Delta}^{(m-)}(x_2) \end{pmatrix} \begin{pmatrix} \mathbf{a}^{(m+)} \\ \mathbf{a}^{(m-)} \end{pmatrix}$$

where $\boldsymbol{\Delta}^{(m\pm)}(x_2)$ and $\mathbf{a}^{(m\pm)}$ correspond to the terms of the matrix $\boldsymbol{\Delta}$ and of the vector **a** relative to reflected (+) and incident (-) partial waves.

By a matter of fact, one can define a reflection matrix $\mathbf{R}^{(m)}$ of rank 4×4 at the interface between layer (*m*-1) and layer *m* linking together incident and reflected partial waves as follows:

$$\mathbf{g}^{(m-)}(X_{m-1}) = \mathbf{R}^{(m)}\mathbf{g}^{(m+)}(X_{m-1}) \tag{3}$$

In case the first layer is semi-infinite, the reflection matrix $\mathbf{R}^{(1)}$ is null, otherwise the bottom surface is assumed free. In this later situation, the surface stress and charge density are assumed null (only the generalized surface displacements in vector **h** are non zero), providing the expression of $\mathbf{g}^{(1)}$. Thus, one can compute the reflection matrix $\mathbf{R}^{(1)}$ considering the definition of (3) [5]. Note that the permittivity of the adjacent medium can be taken into account along the process described in [6]. Once the reflection matrix is known at the first interface, the reflection matrices at the other interfaces of the stack are computed iteratively using a recurrence process. It consists first in linking the interfaces between layers *m* and (*m*+1) via the variable **g** as follows:

$$\mathbf{g}^{(m)}(X_m) = \boldsymbol{\Delta}(-t_m)\mathbf{g}^{(m)}(X_{m-1}) \tag{4}$$

where t_m is the thickness of the layer *m* in conformity with Figure 2. Using (3) allows to express $\mathbf{g}^{(m)}(X_m)$ only as a function of reflected partial waves, yielding the following expression:

$$\mathbf{g}^{(m)}(X_m) = \begin{pmatrix} \mathbf{I}_4 \\ \boldsymbol{\Delta}^{(m-)}(-t_m)R^{(m)}\boldsymbol{\Delta}^{(m+)}(t_m) \end{pmatrix} \boldsymbol{\Delta}^{(m+)}(-t_m)\mathbf{g}^{(m+)}(X_{m-1}) \tag{5}$$

In (5), $\mathbf{I}_4$ is the identity matrix of rank 4×4. The continuity of the generalized normal stresses and displacements at the interface between layers *m* and (*m*+1), i.e. the equality of state vectors $\mathbf{h}^{(m+1)}(X_m)$ and $\mathbf{h}^{(m)}(X_m)$, provides the relation between $\mathbf{g}^{(m+1)}$ and $\mathbf{g}^{(m)}$ which reads:

$$\mathbf{g}^{(m+1)}(X_m) = \left[\mathbf{F}^{m+1}\right]^{-1}\mathbf{F}^{(m)}\mathbf{g}^{(m)}(X_m) \tag{6}$$

Equation (5) can be now inserted in (6), yielding the definition of a matrix of rank 8×4 in which two sub-matrices **K** and **L** can be emphasized, relative to reflected and incident partial waves of layer (*m*+1) respectively:

$$\left[\mathbf{F}^{m+1}\right]^{-1}\mathbf{F}^{(m)}\begin{pmatrix} \mathbf{I}_4 \\ \boldsymbol{\Delta}^{(m-)}(-t_m)\mathbf{R}^{(m)}\boldsymbol{\Delta}^{(m+)}(t_m) \end{pmatrix} = \begin{pmatrix} \mathbf{K} \\ \mathbf{L} \end{pmatrix} \tag{7}$$

In conformity with (3), one can finally deduced the reflection matrix of layer (*m*+1) as $\mathbf{R}^{(m+1)}=\mathbf{L}\mathbf{K}^{-1}$. This iterative scheme is repeated until the top layer of the stack is reached (i.e. $x_2 = X_N$ as defined in Figure 2). The state vector **h** relative to the top surface then reads:

$$\mathbf{h}(X_N) = \mathbf{F}^{(N)}\mathbf{g}^{(N)}(X_N) = \mathbf{F}^{(N)}\begin{pmatrix} \mathbf{I}_4 \\ \boldsymbol{\Delta}^{(N-)}(-t_N)\mathbf{R}^{(N)}\boldsymbol{\Delta}^{(N+)}(t_N) \end{pmatrix}\mathbf{g}^{(N+)}(X_N) = \begin{pmatrix} \mathbf{N} \\ \mathbf{P} \end{pmatrix}\mathbf{g}^{(N+)}(X_N) \tag{8}$$

Introducing **N** and **P** as sub-matrices relative to the generalized surface displacements and stresses respectively, one can define the spectral Green's function relating u_i to T_{2j} as $\mathbf{G}=\mathbf{N}\mathbf{P}^{-1}$ (where **G** is a 4×4 rank matrix), in conformity with the usual process for semi-infinite substrates [7]. We use here the results obtained via the reflection matrix as defined in (3) to characterize the efficiency of the Bragg mirror to design.

An example of computation results is reported in Figure 3 for a Bragg mirror built using an alternation of Lithium Tantalate and Quartz layers allowing for an acoustic impedance difference in excess of 3. It turns out that for 4 layer pairs in the 10 MHz region, the mirror actually operates as expected, yielding a stop-band of about 8 MHz considering fast or slow shear wave. Note also that the mirror exhibit a wider stop-band for the longitudinal wave which could be of interest for other applications.

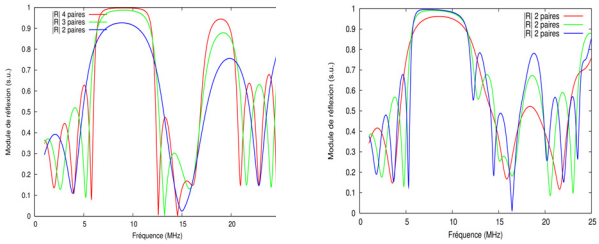

(a) Shear (b) Longitudinal

Figure 3: Computation results of reflection coefficient for a Lithium Tantalate/Quartz Bragg mirror, efficiency of the reflection vs number of layer pairs

The fabrication of such a mirror is now made possible by the recent development in our laboratory of a process for bonding and thinning wafers, so called "WoW", an acronym for "Wafer on Wafer". This process will be described in the next paragraph, followed by its application to the fabrication of a first prototype of acoustic Bragg mirror designed to work at a frequency of 10MHz.

4 Fabrication Process

4.1 WoW (Wafer on Wafer)

The fabrication process has already been presented in details [8], thus we will only summarize the main steps here (Figure 4). A major interest of this process is that wafers of any materials can be bonded together. In particular in the field of acoustic, it is very advantageous to have the possibility to choose various materials with various properties and configurations to create innovative devices and functions. For instance this process has been used to fabricate HBAR (High-overtone Bulk Acoustic Resonators) that were used for different applications such as oscillators [9][10], filters [11] and gas [12] and pressure [13] sensors.

The only requirements for the wafers are that they have a well polished surface, ideally of optical quality, and a low TTV (Total Thickness Variation), to favour the bonding. The first step is the cleaning of the wafers and then the deposition of a Chromium and Gold layer by sputtering. The cleaning is very important as any dust or trace will lead to bonding default. Thus, additionally to classical solvent and acid wet cleaning, we added a cleaning step both before and after sputtering that use a megasonic cleaner (CL200 from Suss Microtec).

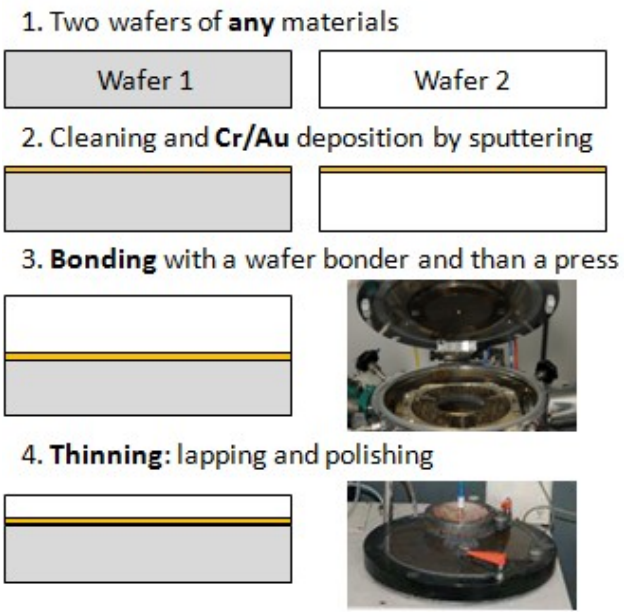

Figure 4: WoW fabrication process

The two wafers are then bonded together under vacuum by thermocompression of the Gold layer, using a wafer bonder. The constraints due to different thermal expansion coefficients of the two materials are minimized by working at room temperature.

The quality of the bonding is non-destructively characterized with a homemade ultrasonic characterization bench. The stack is immersed in a water tank and the whole bonded surface is scanned with a focalized acoustic beam, by using tow focalized transducers. The transmission of the beam is measured and the defects appear clearly in the scan as they reduce transmission. The lateral resolution is about 200µm, corresponding to the diameter of the focalised acoustic beam.

Using this characterization tool we understood that the bonding by the wafer bonder was often incomplete. So we developed an additional step using a press that could use much higher pressure and the characterization has shown a clear improvement or the quality of the bonding. Now, bonding of more than 95% of the surface is commonly achieved.

One of the wafers is subsequently thinned by lapping and polishing to thicknesses as low as 10 microns. The main difficulty is to keep the thickness homogeneous over the surface. For this purpose, we have developed a special holder using three micrometer screws that enable us to obtain homogeneities of typically ±5µm.

By using this process we were able to fabricate a first demonstrator of an acoustic Bragg mirror as described in the next paragraph.

4.2 Fabrication of the Bragg mirror

The mirror is composed of 4 double-layer of lithium tantalate (LT) (YXl)-42° on quartz (Q) (YXl)-35,5°. The nominal thicknesses are respectively 105µm and 87µm for reflection at 10MHz (Figure 5a). On top of the mirror is bonded the resonator itself which is a 500µm thick wafer or quartz (YXl)34°. A silicon wafer is used as the holder for the device.

During the fabrication, the wafers were successively bonded and thinned from the bottom of the stack to the top. As a consequence, the defects were adding up with each new bonding as it appears clearly on the ultrasonic characterization (Figure 6).

Nevertheless we were able to obtain a stack of ten wafers with some parts presenting good quality enough to show evidence of the Bragg mirror effects as we will show in the next section. At the end of the process, the wafer was diced in order to characterize the stack with a scanning electronic microscope (SEM). A SEM view is presented in Figure 7.

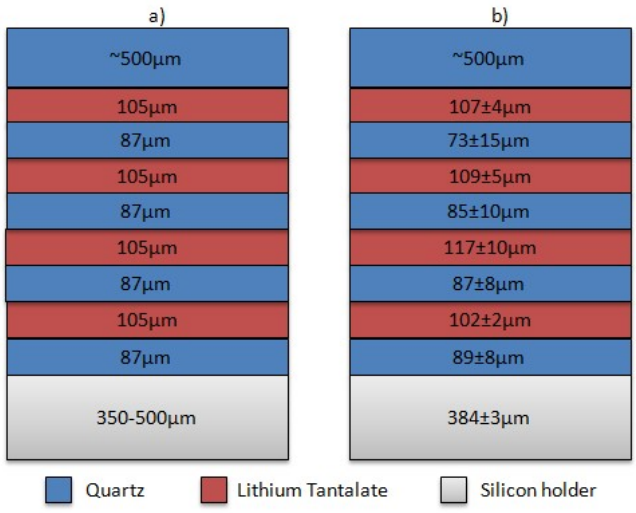

Figure 5: Bragg mirror stack with the nominal thicknesses (a) and the actual thicknesses after fabrication (b)

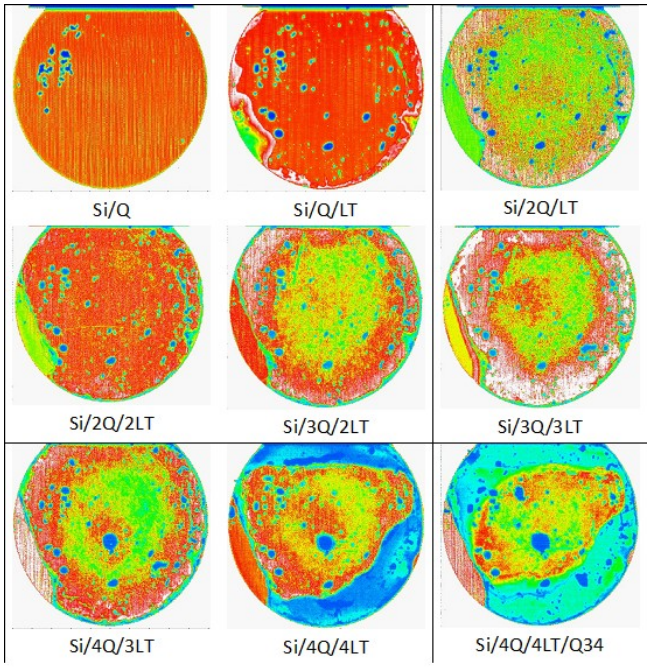

Figure 6: Ultrasonic characterisation of the stack for each new wafer added. The colours representing the best quality and lowest quality bonding are respectively red and blue.

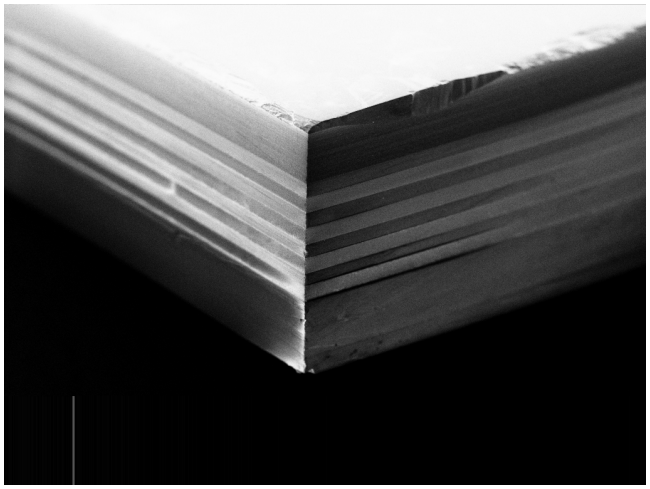

Figure 7: SEM view of the Bragg mirror. The silicon holder is at the top and the quartz resonator at the bottom.

5 Characterization

To check the functionality of the mirror, we used our acoustic characterization bench. Indeed, the frequency of the signals produced by the focalized transducer is 15MHz which is close to the working frequency of our Bragg mirror. After measuring the transmission and reflection in the time domain, we could obtain a spectrum in the frequency domain by applying a Fourier Transform. This measurement was performed for each new double LT/Q added to the stack, and the results are presented on Figure 8.

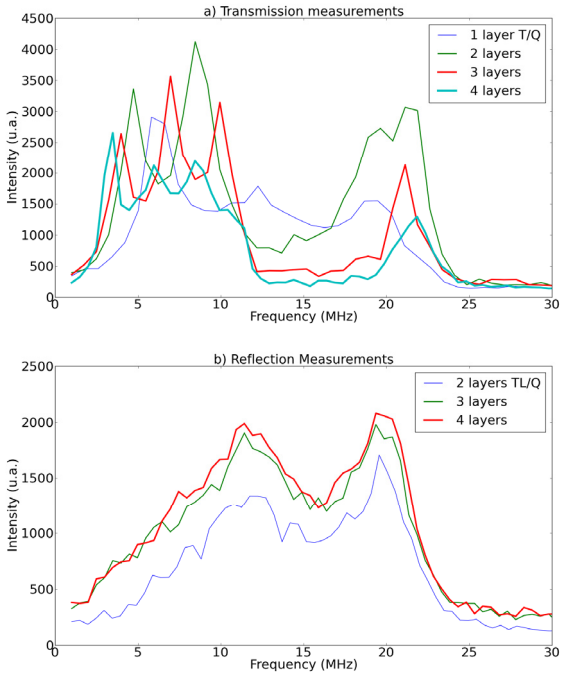

Figure 8: Transmission (a) and reflection (b) spectra of 1, 2, 3 and 4 double layer of Q/TL (reflection for 1 double layer was not measured)

Each curve corresponds to an average over 26 measurements at different locations. The effect of the Bragg mirror appears clearly in the transmission spectrum. There is a frequency range, from about 12 to 20MHz, in which the transmission is reduced, and this reduction gets clearer for each new layer added. We also observe two peaks of reflection at about 12MHz and 20MHz.

After the characterization of the mirror, we added the resonator by using the same WoW process. The thickness of the resonator was fixed to 500µm in order to have the third mode close to 11.6MHz. Several resonators were fabricated on the wafers stack by a batch process. A 200nm thick Cr/Au layer was sputtered and structured by a liftoff process in clean room to define the top electrodes. They had a circular shape, with a diameter varying from 5 to 8mm and with a connection pad at one side (Figure 9a). The bottom electrode was provided by the bonding gold layer between the mirror and the resonator wafer.

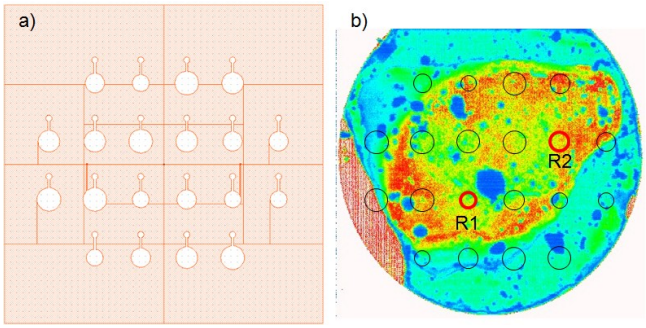

Figure 9: a) Mask used to fabricate the resonators electrodes; b) Position of the resonators on the stack. R1 and R2 were measured.

The admittance was measured with a network analyser for two of the resonators named R1 and R2. Their position on the mirror is shown on Figure 9b. We obtained a mode

around 9.9MHz. We were expecting the mode at 11.6MHz, right at the maximum reflection of the mirror. We understood that we used the wrong speed in the calculation of the frequency. When using the correct speed, we find the same frequencies for the calculation and the experiments for the 4 modes measured. Nevertheless, at 9.9 MHz, we are still at a high reflection level of the Bragg mirror. The admittance curves for this mode, for the resonators R1, R2, and a reference resonator made on a single wafer of quartz are presented on Figure 10.

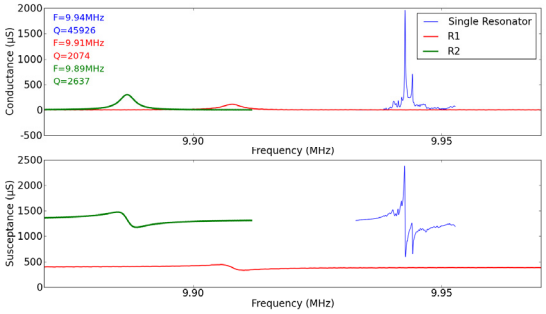

Figure 10: Admittance for two resonators on the Bragg mirror (R1 and R2) and a reference resonator on a single wafer

The resonator R2 shows a factor quality Q of 2637, which is better than the Q of R1 (2074). This could be explained by the fact that R2 is situated at a position on the Bragg mirror presenting fewer defects than the position of R1 (Figure 9b).

6 Conclusion and perspectives

We have demonstrated the feasibility of an acoustic Bragg mirror working at a frequency of 10MHz. The fabrication was achieved using a WoW process based on bonding and thinning of wafers. The design of the mirror, especially the choice of material and the configuration (thickness, cut angles) was done based on the simulations. By acoustic measurements, the effect of the Bragg mirror was clearly demonstrated. Resonators were bonded to the mirror and the admittance was measured, showing a quality factor of about 2600. The value of the quality factor depends on the quality of the Bragg mirror.

Now we are working on a new demonstrator. The procedure for the fabrication of the mirror was modified. Each double-layer LT/Q is first bonded and the quartz is thinned before being added to the stack. By this way, if one of the double-layer present too many defects, it can be replaced by a new one, thus we have less chance that a single poor bonding affect the quality of the whole stack. Moreover we have improved the quality of our lapping and polishing steps. Thus we expect to obtain better quality Bragg mirror and consequently better quality factors for the resonators bonded on the mirror.

References

[1] W.E. Newell, “Face mounted piezoelectric resonatore”, Proc. of the IEEE, pp. 575-581, 1965

[2] D. Gachon, E. Courjon, G. Martin, L. Gauthier-Manuel, J.-C. Jeannot, W. Daniau and S. Ballandras, “Fabrication of high frequency bulk acoustic wave resonator using thinned single-crystal Lithium Niobate layers”, Ferroelectrics, 362:30-40, 2008

[3] A. Reinhardt, « Simulation, conception et réalisation de filtres à ondes de volume dans des couches minces piézoélectriques », PhD. Thesis at University of Franche-Comté, Besançon, 2005

[4] E. L. Adler, “Matrix methods applied to acoustic waves in multilayers”, IEEE Trans. on UFFC, Vol. 37, N°2, pp. 485-490 (1990).

[5] Th. Pastureaud, V. Laude, S. Ballandras, “Stable scaterring matrix method for surface acoustic waves in piezoelectric multilayers”, Appl. Phys. Lett., Vol. 80, pp. 2544-2546, 2002

[6] A. Reinhardt, Th. Pastureaud, S. Ballandras, V. Laude, “Scattering matrix method for modeling acoustic waves in piezoelectric, fluid and metallic multilayers”, Journal of Appl. Phys., Vol. 94, N°11, 2003

[7] P. M. Smith, “Dyadic Green’s function for multilayer substrates”, IEEE Trans. on UFFC, Vol. 48, pp.171 (2001)

[8] T. Baron et al, “Temperature compensated radio-frequency harmonic bulk acoustic resonators, Proc. Of the IEEE IFCS, pp. 652-655, 2010.

[9] E. Lebrasseur, G. Martin, D. Gachon, T. Baron, A. Reinhardt, P.-P. Lassagne, L. Chommeloux, S. Ballandras, “A Feedback-Loop Oscillator Stabilized Using Laterally-coupled-mode Narrow-band HBAR Filters”, IEEE International Ultrasonics Symposium (IUS) 2011

[10] F. Bassignot, E. Lebrasseur, G. Ulliac, G. Martin, E. Courjon, B. François, J.-M. Lesage, S. Ballandras, “Silicon/Periodically Poled Transducer/Silicon resonant devices for the stabilization of RF oscillators”, IEEE International Ultrasonics Symposium (IUS) 2011

[11] D. Gachon, T. Baron, G. Martin, E. Lebrasseur, E. Courjon, F. Bassignot, S. Ballandras, “Laterally coupled narrow-band high overtone bulk wave filters using thinned single crystal lithium niobate layers”, Frequency Control and the European Frequency and Time Forum (FCS), 2011

[12] D. Rabus, T. Baron, E. Lebrasseur, S. Alzuaga, G. Martin, S. Ballandras, J.-M. Friedt, “Novel Narrowband Acoustic Sensors for Sub-GHz Wireless Measurements” IEEE Sensors 2011, pp. 1309-1312

[13] T. Baron, E. Lebrasseur, J.P. Romand, S. Alzuaga, S. Queste, G. Martin, D. Gachon, T. Laroche, S. Ballandras, J. Masson, “Temperature compensated radio-frequency harmonic bulk acoustic resonators pressure sensors”, IEEE Ultrasonics Symposium (IUS) 2010, pp. 2040-2043.